Methods 46 (2008) 104–115

Contents lists available at ScienceDirect

Methods

journal homepage: www.elsevier.com/locate/ymeth

Probing the function of ionotropic and G protein-coupled receptors in surface-confined membranes

Christophe Danelon [a], Samuel Terrettaz [a], Olivier Guenat [b], Milena Koudelka [b], Horst Vogel [a,*]

[a] Laboratory of Physical Chemistry of Polymers and Membranes, Ecole Polytechnique Fédérale de Lausanne (EPFL), CH-1015 Lausanne, Switzerland
[b] Sensors, Actuators and Microsystems Laboratory, Institute of Microtechnology, University of Neuchâtel, Rue Jaquet-Droz 1, CH-2002 Neuchâtel, Switzerland

ARTICLE INFO

Article history:
Accepted 2 July 2008
Available online 26 July 2008

Keywords:
Supported membrane
Impedance spectroscopy
Ion channel
Membrane receptor
Planar lipid bilayer
Fluorescence microscopy
Surface-sensitive technique
Cellular signaling
Functional assays
Biosensors

ABSTRACT

This article reports on recent electrical and optical techniques for investigating cellular signaling reactions in artificial and native membranes immobilized on solid supports. The first part describes the formation of planar artificial lipid bilayers on gold electrodes, which reveal giga-ohm electrical resistance and the insertion and characterization of ionotropic receptors therein. These membranes are suited to record a few or even single ion channels by impedance spectroscopy. Such tethered membranes on planar arrays of microelectrodes offer mechanically robust, long-lasting measuring devices to probe the influence of different chemistries on biologically important ionotropic receptors and therefore will have a future impact to probe the function of channel proteins in basic science and in biosensor applications. In a second part, we present complementary approaches to form inside-out native membrane sheets that are immobilized on micrometer-sized beads or across submicrometer-sized holes machined in a planar support. Because the native membrane sheets are plasma membranes detached from live cells, these approaches offer a unique possibility to investigate cellular signaling processes, such as those mediated by ionotropic or G protein-coupled receptors, with original composition of lipids and proteins.

1. Introduction

The plasma membrane at the interface between exo- and cytoplasm of a biological cell processes a network of signaling reactions which are of central importance for the functioning of a cell. In spite of intensive research, many key questions remain unsolved, for example (i) how chemical and physical signals are sensed by particular membrane proteins, (ii) how these membrane proteins process the signals by a complex biochemical network of interacting proteins, (iii) how these processes are modulated by highly dynamic spatiotemporal concentration changes of membrane lipids and in turn membrane proteins, and (iv) how these reactions on the membrane couple to the biochemical signaling network inside of the cell, Reviews: [1–5]. A detailed insight into these themes will have also a large impact to understand and treat diseases [6].

Often these questions have been addressed using model membranes to simplify the complexity of living cells [7]. Although classical biophysical and bioanalytical means are dominating in this field, there are emerging micro-, nano- (single-molecule) techniques, which open new vistas for investigating and thereby delivering important insights into the functions of membranes unattainable by traditional methods [8]. Examples are the detection of structural fluctuations of membrane proteins under physiological conditions using scanning probe and single molecule optical microscopies [9,10], the monitoring of the folding/unfolding of single membrane proteins by force microscopies and optical spectroscopies [11,12], the observation of trajectories of single protein and lipid molecules visualizing membrane microdomains by single molecule optical microscopy [13]. Many of these techniques rely on membranes or membrane components immobilized on solid supports.

Historically, supported membranes were first used in the 1980s by Harden McConnell and his colleagues to investigate molecular processes and simulate cell–cell interactions of the immune system by fluorescence microscopy and total internal reflection [14]. Planar membranes were formed either as lipid monolayers on alkylated glass plates [15] or as lipid bilayers on hydrophilic (mostly glass) supports either by successive transfer of monolayers from the air–water interface to the support [16] or by fusing lipid vesicles from an aqueous bulk phase to a hydrophilic glass slide [17]. These developments were the basis for many forthcoming biophysical investigations on artificial planar supported membranes [18–22].

In parallel there was in the 1980s a growing interest to use surface immobilized biological molecules (mostly water-soluble redox-enzymes, antibodies, DNA) to detect and quantify analytes

* Corresponding author. Fax: +41 21 693 6190.
E-mail address: horst.vogel@epfl.ch (H. Vogel).

1046-2023/$ - see front matter © 2008 Elsevier Inc. All rights reserved.
doi:10.1016/j.ymeth.2008.07.004

by biosensors [23–26]. In the 1990s the biosensing concept was extended to membrane proteins. In order to obtain mechanically robust and electrically insulating membranes comprising functionally active membrane receptor proteins novel methods have been developed to tether lipid bilayers covalently to solid supports (gold, glass, silicon/SiO2) either via hydrophilic spacers [27–29], on a nanometer-thick polymer cushion [30] to create a water film between the lipid bilayer and the sensor surface and thereby ensure the functional integrity of the reconstituted membrane proteins, or later by tethering the membrane to the solid support by the functional transmembrane protein to be investigated [31,32]. Based on these original concepts, many groups have since reported different tethered lipid bilayers either in pure form or with integrated polypeptides or large membrane proteins, Reviews: [33–38].

The large potential of tethered supported membranes as a generic bioanalytical platform became only evident from reports that demonstrate specific dose-dependent functional activation of reconstituted transmembrane proteins, such as membrane-integrated enzymes and transporters, GPCR-mediated signaling, and ligand-gated ion channels:

(i) In the case of membrane-integrated enzymes, Naumann et al. have shown in tethered membranes the reconstitution of ATPase activity for F_0F_1ATPase [29], proton transport and electron transfer for cytochrome oxidase [39] and proton translocation for H^+ATP synthase [40].

(ii) A different approach to probe activities of membrane transport proteins was developed by Seifert et al. [41]: These authors used lipid monolayers on self-assembled thioalkane monolayers on gold surfaces onto which they adsorbed lipid vesicles with reconstituted membrane transporters. Although the state of the adsorbed vesicles was not totally resolved (flattened vesicles or single/multiple lipid bilayer sheet/s), the reported transient current measurements reflect transport processes of the reconstituted membrane proteins. This method has been optimized over the years for probing membrane transport processes of relevance in drug discovery [42].

(iii) A prototypical G protein-coupled receptor, rhodopsin, was reconstituted in patterned tethered lipid bilayers together with its G protein; activation of the receptor and its downstream G protein could be monitored in situ in a dose–response manner using surface plasmon resonance imaging [31,43]. These two reports are of general importance because they demonstrate that complex cellular signal transduction processes can be reconstituted in micropatterns of tethered membranes that serve as a platform for screening the function of GPCRs in a multiarray format. Because GPCRs represent the largest class of membrane proteins and are among the most important targets for therapeutical compounds, this biosensor approach opens new possibilities in drug screening and for studying interactions between membrane proteins involved in complex cellular signaling reactions.

(iv) The dose dependent activation of ligand-gated ion channels have been measured in highly insulating tethered membranes on conducting electrodes for a number of native and artificial ion channels. First, selective binding of an antibody to its antigen sequence, chemically ligated to the small peptide ionophore Gramicidin, has been shown to modulate sensitively the Gramicidin-mediated ion channel activity; this is the basis for a novel electrical immunosensor [44]. Second, the channel-forming protein OmpF from the outer membrane of *Escherichia coli* was reconstituted into tethered membranes on gold electrodes. The selective binding of a fragment of colicin N protein to the extracellular part of OmpF, determined by surface plasmon resonance (SPR), closed the channel in a dose-dependent manner as monitored by simultaneous impedance measurements on the gold-electrode-tethered membranes and by complementary ion current measurements on BLMs [45]. This is to our knowledge the only case where modulation of ion channel activity in a native transmembrane protein has been demonstrated in tethered membranes. Third, a fully synthetic ligand gated ion channel (SLIC) was synthesized composed of four transmembrane, channel forming amphipathic segments, four N-terminal antigenic $(NANP)_3$ sequences and a hydrophilic branched polypeptide serving as a spacer between the C-terminal sulphur attached to the gold electrode and the lipid bilayer, which can be assembled around the central part of the SLIC. Selective binding of a monoclonal antibody against the extramembraneous NANP-sequence revealed a concomitant modulation of the ion channel activity in an antibody concentration-dependent manner [32,46]. SLIC in tethered membranes on conducting electrodes offers a very versatile platform to detect sensitively an analyte of interest that can selectively bind to a molecular recognition element covalently ligated to the channel entrance and thereby capable to gate the ion channel activity of SLIC.

Our article concerns experimental details on recent surface sensitive electrical and optical techniques for investigating cellular signaling reactions in artificial and native membranes tethered to solid supports as outlined in Fig. 1.

The first part of our article describes the formation of planar artificial lipid bilayers on gold electrodes and their use for measuring the activity of ion channel proteins with impedance spectroscopy. An additional very promising development for the future is the possibility to combine the electrical impedance measurements with other surface sensitive techniques such as quartz crystal microbalance, SPR, SPR excited fluorescence or scanning probe techniques.

The second part of our article concerns a complementary approach to form planar membranes that are tethered to a solid support but in addition span (multi-arrayed) micrometer- to nanometer-sized holes machined in this support. Elsewhere, we have reported how to produce by electrophoretic self-positioning across single holes totally solvent-free artificial planar lipid bilayers, which are ideally suited for reconstituting and measuring single ion channels by so-called planar patch-clamping [47]. Here, we will describe the production of planar native membrane sheets across holes in the solid support and their use for optical and electrophysiological measurements. Because the native membrane sheets are plasma membranes detached from live cells, this approach offers a unique opportunity to access (adding active compounds or membrane components via the fluidic phase, orthogonal modifying/labeling different membrane components) both the exo- and the cytoplasmic site of a cellular membrane under physiological conditions, which cannot be realized in a living cell. Because these planar membrane sheets can be probed by optical and electrical means, this opens new possibilities to investigate cellular signaling processes with single molecule resolution.

2. Description of methods

2.1. Lipid membranes tethered to gold electrodes

Phospholipid bilayers chemically bound to gold surfaces are obtained by self-assembly of sulphur containing synthetic lipids. These so-called thiolipids are phospholipids comprising at their polar head groups a hydrophilic spacer, which is terminated by a –SH group (Fig. 1A) [28,43,44,48]. The hydrated spacer decouples the lipid bilayer from the gold surface. The resulting aqueous film between the electrode surface and the lipid bilayer has been designed to accommodate extracellular parts of transmembrane proteins. G protein-coupled receptors and ion channels have been reconstituted in a functionally active form into these gold supported lipid bilayers [31,32,43,45].

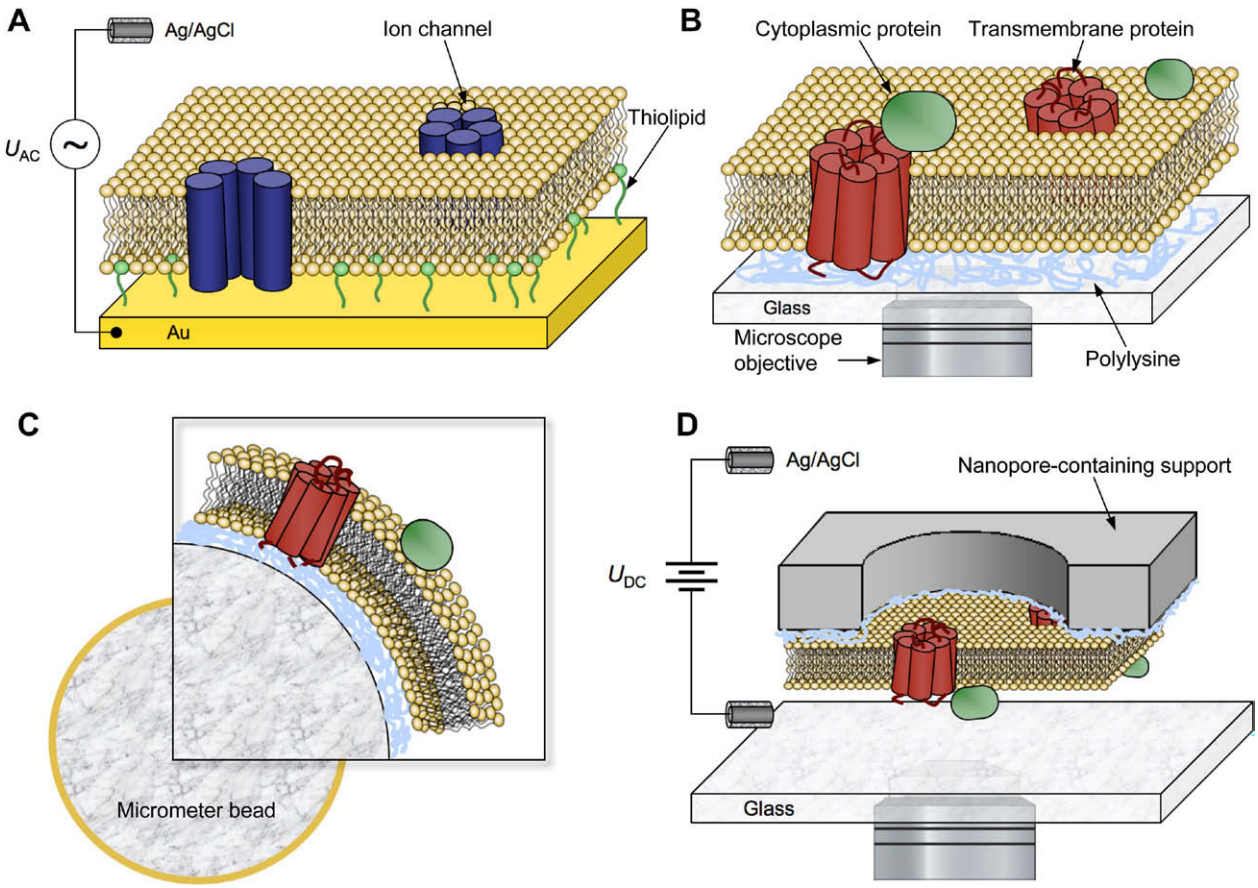

Fig. 1. Cartoon illustrating the different configurations of supported membranes presented in this article. (A) Ion channel-containing lipid bilayer tethered to a working gold electrode via synthetic thiolipids. (B–D) Inside-out membrane sheets detached from living cells can be immobilized on various solid supports, such as (B) planar glass slides, (C) micrometer-sized beads, and (D) supports comprising nanopore arrays. Membrane properties can be investigated optically (A–D) or electrically (A,D).

2.1.1. Preparation of giga-ohm resistance membranes on millimeter-sized gold electrodes

Glass slides were cleaned by ultrasonication first in; 2% detergent solution (Hellmanex Hellma, Germany) and then in pure water. Electrodes of 1 mm diameter were prepared by vapour deposition of 50 nm thick gold films through a metallic mask on the glass under vacuum (5×10^{-6} mbar). Adhesion of gold to the glass surface was improved either by deposition of an intermediate 1 nm thick chromium layer or by silanization of the glass surface with 3-mercaptopropyltrimethoxy-silane. After cooling to room temperature, the gold-coated glass slides were transferred to a freshly prepared thiolipid solution (1 mg/mL) in buffer A (48 mM octylglucoside, 0.1 M KCl/sodium phosphate buffer at pH 7.4) for at least 1 h. During this incubation period, a thiolipid monolayer was formed at the gold surface. After washing the electrode covered with the thiolipid monolayer with buffer A, a second monolayer of phospholipids was formed as follows: the electrode was first incubated in a solution of 1 mg/mL phospholipids (e.g. POPC, DOPC or dPhyPC) in buffer A, which was then diluted stepwise below the critical micellar concentration (CMC) of the detergent [49].

In order to get highly insulating bilayers with membrane resistances close to 1 GΩ, overnight incubation in a solution containing a thiolipid consisting of a single phytanoic acid coupled to a hydrophilic spacer was performed [46]. The lipid bilayer was then completed by a monolayer of dPhyPC/cholesterol (9:1) using the detergent dilution technique described above. Our concept to tether lipid bilayers via –SH terminated oligoethylene spacers to gold surfaces was since then also used by others to realize highly electrically insulating membranes on ultraflat gold surfaces [50].

2.1.2. Preparation of giga-ohm resistance membranes on micrometer-sized gold electrodes

Our rationale to form tethered membranes on microelectrodes is twofold. First, microelectrodes are expected to increase the time resolution of channel measurements. Second, individually addressable microelectrodes will allow the formation of arrays of self-assembled tethered membranes with distinct composition, i.e. screening the function of different membrane proteins in a highly parallel format.

Here, we report on the production of micrometer-sized gold electrodes (Fig. 2) and their application for impedance measurements of tethered membranes. The use of glass as an insulating support (instead of silicon) and the miniaturization of the electrical connections were essential to reduce the stray capacitance of the working electrode below 10 pF, a prerequisite to allow impedance measurements of tethered membranes on electrodes as small as 50 μm in diameter.

A 50 μm window was photolithographically produced in a passivation layer deposited on top of gold electrodes of 55 and 60 μm diameters. We used slightly oversized microelectrodes to compensate the photolithographic alignment limitations. The diameter reduction of the second type of microelectrode was intended to limit the parasitic capacitance produced by the underlying passivated microelectrode periphery. The first microelectrode was connected with a 725-μm long and 10-μm wide gold track, while the smaller microelectrode was connected with a 500-μm long and 6-μm wide gold track. Both connections widen up at 200 μm until reaching the contact pad after 2.6 mm (Fig. 2). The reduction of the surface between the two microelectrodes (500 μm track length) was estimated to reduce the parasitic stray capacitance by 40%.

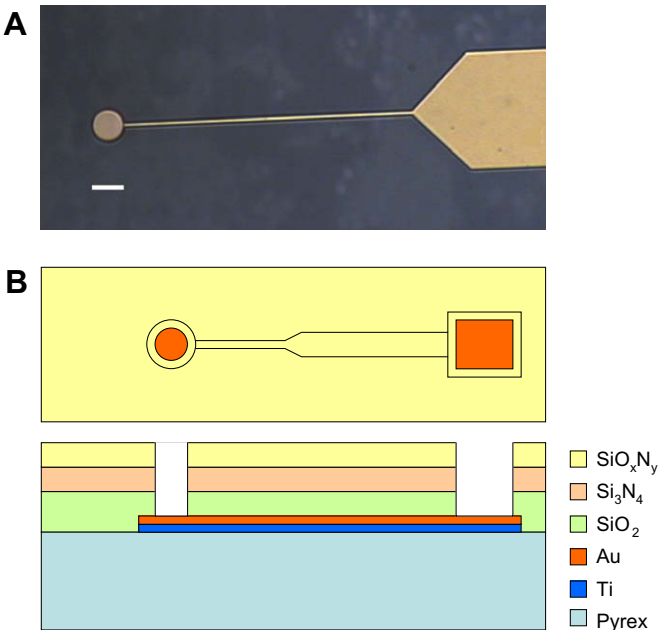

Fig. 2. (A) Photograph of a 50-μm disk gold electrode with its electrical connection track. (B) Scheme of top view and cross-section of a 50-μm microelectrode shown in (A) with narrow connecting track to a square pad (drawing is not to scale). These electrodes show very low stray capacitance due to (i) thick passivation layers, (ii) narrow connecting tracks and (iii) the use of a glass support. The maximal length of the connecting tracks in the electrochemical cell was set to approximately 50 μm by an O-ring.

The microelectrode shown in Fig. 2 was fabricated using photolithography. Briefly, 70 nm thick gold disk electrode and track connection were patterned by a lift-off process together with a 50 nm titanium adhesion layer onto a 0.5-mm thick Pyrex glass plate. Different thin dielectric layers were deposited successively instead of producing one single thick passivation layer, in order to avoid the intrinsic stress of thick layers. 600 nm thick SiO_2, 400 nm thick Si_3N_4 and 400 nm thick SiO_xN_y layers were deposited successively by plasma-enhanced chemical vapour deposition. The windows on the microelectrodes and on the connection pad were produced by photolithography. The three passivation layers were etched in 7:1 buffered HF.

The gold microelectrodes were cleaned by local application of hot chromic acid (saturated potassium dichromate in concentrated sulphuric acid) on the glass chip. Piranha solution (2:3 H_2O_2/H_2SO_4) can be used instead of chromic acid. The electrodes were rinsed thoroughly with water, dried with a stream of nitrogen and sealed at the bottom of the cell by means of an O-ring. The electrodes were then left for 15 min in ethanol in order to remove the labile gold oxide and washed again with water. Tethered planar membranes were formed as described in Section 2.1.1.

2.1.3. Characterization of tethered lipid membranes by impedance spectroscopy

The real and imaginary parts of the impedance spectrum of a tethered lipid bilayer on a microelectrode in aqueous solution are shown in Fig. 3A. The data can be fitted by the equivalent circuit depicted in the inset of Fig. 3A. The electrical parameters of the lipid bilayer membranes are classically modelled by a capacitance C_M and a resistance R_M in parallel. The capacitance describes the dielectric properties of the electrically insulating lipid bilayer sandwiched between two conductive phases, namely the gold electrode and the electrolyte. The resistance critically depends on electrically conducting defects in the lipid membrane. In the impedance spectrum, the intrinsic parameters of the lipid bilayer can often be separated from other elements of the electrochemical cell such as the interfacial capacitance C_I, the charge transfer resistance at the gold/electrolyte interface R_{CT} and the electrolyte resistance R_S [51]. From 18 measurements, we obtained a membrane capacitance value of $1.05 \pm 0.20\,\mu F/cm^2$, which was slightly higher than the value of $0.6 \pm 0.1\,\mu F/cm^2$ determined on larger electrodes [46,52]. This higher capacitance value may be explained by the influence of the stray capacitance of microelectrodes. The membrane resistance of tethered membranes on microelectrodes was in the order of $R_M = 10\,G\Omega$. In Fig. 3A the membrane resistance is graphically obtained from the plateau of the real part of the impedance Z_r in the frequency range between 0.1 and 1 Hz.

Fig. 3B shows the real part of the impedance spectrum of lipid bilayer membranes tethered to millimeter and micrometer-sized electrodes. By optimizing the (thio)lipid composition, tethered lipid bilayers of $R_M = 2 \times 10^8\,\Omega$ have been obtained on 1 mm diameter gold electrode (Fig. 3B, dotted line), which was close to corresponding R_M values of freestanding planar lipid bilayer membranes (BLM) used for classical single-channel conductance measurements [46]. Lipid bilayer membranes with low defect densities have been produced in order to increase the sensitivity of the impedance measurements and to suppress interference with non-specific adsorption.

The improvement of membrane resistance however increases also the time constant of the membrane R_MC_M and shifts the measuring range of the resistance to lower frequencies. The modulation of the membrane resistance should therefore be measured in the same frequency range with a low time resolution. The spectral shift of the plateau of Z_r from 100 Hz to 10^{-2} Hz with a 10,000-fold increase of membrane resistance is shown for a lipid bilayer on a 1-millimeter-sized gold electrode (Fig. 3B, dotted vs. dashed line). A lower time constant was obtained by reducing the membrane capacitance using microelectrodes. While the capacitance value scales with the surface area, the resistance value of a tethered lipid bilayer depends primarily on the number and nature of the defects and does not follow a simple relation with the surface geometry. As a result, the time constant of the tethered lipid bilayer (unlike bulk material) depends on the electrode geometry. For this reason, we do not recommend to normalize measured values of the membrane resistance by the electrode surface area as often found in the literature. Here, we report on planar lipid bilayers tethered

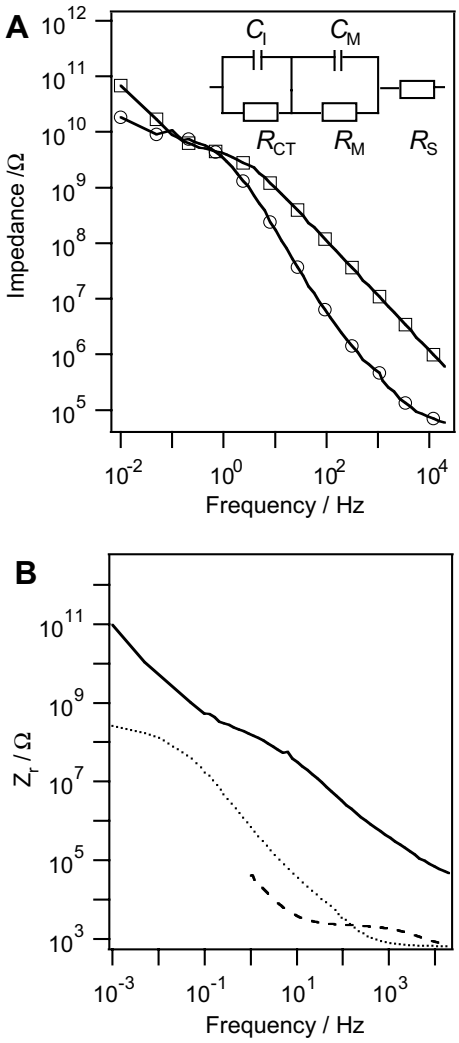

Fig. 3. (A) Real (○) and imaginary (□) part of the impedance spectrum of lipid bilayer tethered to a 50-μm diameter gold electrode in 0.1 M KCl, 5 mM phosphate buffer, pH 7.4. 50 points were measured equally spaced on a log scale from 0.1 Hz to 20 kHz; every 5th point is shown, together with two additional points measured at 0.01 and 0.05 Hz. The charge-transfer resistance of the gold/water interface R_{CT} and the resistance of the lipid bilayer membrane R_M and of the electrolytic solution R_S are spectrally well resolved. C_M and C_I denote the capacitance of the lipid bilayer membrane and the interface, respectively. The electrical resistance R_M of the bilayer can be obtained from the difference between the values of Z_r in the plateau region (0.1–1 Hz) and at high frequencies. In the example shown the membrane resistance was $R_M = 10\,G\Omega$. (B) Real part of the electrical impedance spectrum of a highly insulating tethered lipid bilayer on a 50 μm diameter microelectrode (continuous line) and on a 1 mm diameter macroelectrode (dotted line). 199 data points were measured equally spaced on a logarithmic scale between 0.1 Hz and 20 kHz together with five additional data points between 10^{-3} Hz and 10^{-1} Hz. The impedance spectrum of an electrically less dense tethered lipid bilayer with the molecular composition previously used for antibody binding to SLIC in tethered lipid bilayer [32] is also shown (dashed line). It is important to note, that for microelectrodes the plateau where the lipid bilayer resistance can be measured directly with little influence from other circuit elements is shifted to frequencies up to approximately 10 Hz resulting in a 100-fold increase of time resolution.

to microelectrodes showing giga-ohm resistances, which can be measured at frequencies of several Hz with a time resolution of less than 1 s (Fig. 3B, continuous line). Recently tethered bilayer lipid membranes with giga-ohm resistances have been measured on gold microelectrodes from 8 to 4000 μm diameter insulated in a polyimide resist. The authors reported that the electrical membrane parameters were dominated by defects at the edge of the membrane [53].

2.2. Ion channels in lipid membranes tethered to gold electrodes

Different protocols have been developed to incorporate membrane proteins into membranes tethered to gold surfaces. Hereafter, we will discuss the preparation of lipid bilayers containing the outer membrane protein OmpF or the synthetic ligand gated ion channel (SLIC). OmpF is a pore-forming protein from the outer membrane of *Escherichia coli* whose conductance can be modulated by binding the bacterial toxin Colicin N [45]. The SLIC molecule we used here comprises four peptides composed of $(NANP)_3$ sequences as highly specific ligand-binding regions and four melittin peptide segments as membrane-spanning, channel-forming parts [32]; channel activity of the SLIC is modulated by binding of a specific antibody to $(NANP)_3$.

2.2.1. Methods for incorporating ion channels in tethered lipid membranes

For inserting ion channel proteins and reconstituting their functional activity in tethered lipid membranes, we followed usually a two-step protocol developed in our laboratory for OmpF [45]. First, a mixed monolayer of thiolipids and a short-chain ω-hydroxy- or carboxy-thioalkane was prepared by coadsorption of both components. The short-chain hydrophilic thiols were used to dilute the anchor-thiolipid molecules laterally and to prevent direct contact and thus denaturation of membrane proteins at the gold surface. Then, OmpF together with DOPC were self-assembled on the gold electrode to complete the tethered membrane. In more detail, the gold electrode was incubated overnight in a mixture of thiolipids and sulfanylpropionic acid at a molar ratio of 2:1. After washing, a solution of 0.5 mg/mL DOPC and 5 μg/mL OmpF in detergent was added for 30 min, followed by a stepwise dilution below the CMC of the detergent [45].

Detergent-solubilized membrane proteins can also be first bound chemically to the gold surface, followed by formation of a lipid bilayer around the proteins. The completed bilayer is tethered to the gold surface either only via the immobilized protein or in addition via thiolipids comprised in the lipid bilayer. For an oriented immobilization, membrane proteins typically comprise functional groups, which selectively bind to a complementary molecular partner on the gold surface. A number of different methods have been reported in this context [26,33,54]. Histidine tags have been used to bind ligand-gated ion channels to surfaces derivatized with nitrilotriacetic groups [55]. GPCRs have been immobilized in a functional active form via biotin-streptavidin interactions, introducing biotin site-selectively on extracellular glycosylation sites of the receptor [31].

In the following we concentrate on covalent immobilization of membrane proteins on gold via –SH of single cysteines engineered site-selectively into the protein. We have shown that this is a powerful strategy for two examples, a mutant protein of OmpF (OmpF-E183C) [52] and a synthetic channel protein SLIC [32]. To avoid denaturation of the proteins, gold electrodes were first coated by a monolayer of a short ω-hydroxythioalkane. SLIC and OmpF were then added from the bulk aqueous phase in the presence of detergent. Subsequently the bilayer was completed by adding a lipid-detergent solution and diluting it below the detergent's CMC.

Alternatively, ion channels such as SLIC and OmpF have also been inserted into a preformed tethered lipid membrane in analogy to protocols used for BLMs (Fig. 4A) [46]. For reconstituting the proteins' channel activities, the density of thiolipid tethers has to be properly adjusted. Since then, this strategy was also used recently by others for incorporating α-hemolysin into membranes tethered to gold electrodes [56].

The orientation of the incorporated protein is well controlled when it is bound selectively to the electrode via adequate interacting partners (as explained before). In the other cases, there is

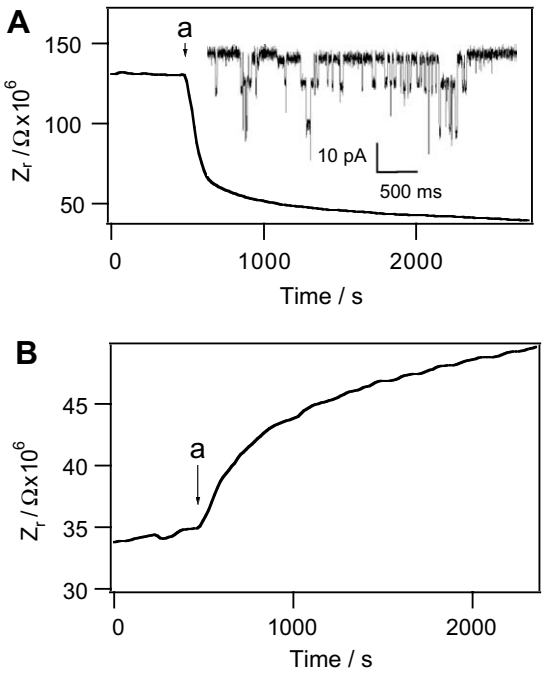

Fig. 4. (A) Time course of the real part of the electrical impedance (measured at 0.01 Hz) of a tethered lipid bilayer after addition (a) of 7×10^{-7} M of SLIC to the aqueous phase. Inset: Single channel recording on a free-standing planar lipid bilayer membrane (BLM) at −30 mV in 1 M NaCl, 10 mM Tris–HCl, pH 7.4. The larger single channel events shown correspond to a conductance level of 90 pS at the buffer conditions used for impedance measurements. (B) Real part of the electrical impedance (measured at 0.01 Hz) of the tethered lipid bilayer containing SLIC after the addition (a) of 10^{-6} M of an antibody binding specifically to the NANP-sequence of SLIC (adapted with permission from reference [46]).

no strict control of the orientation of the membrane proteins. Very likely, the asymmetry of our system (small reservoir between the electrode and the membrane) favors the outside-out orientation of proteins comprising a large extracellular and a small intracellular part as in the case of OmpF. This was, however, never investigated precisely for supported membranes because proteins in the "wrong" orientation cannot be ligand-gated; they merely behave as passive proteins that do not affect the measurements at low concentrations.

2.2.2. Probing ion channel activity in lipid membranes tethered to gold electrodes

An unequivocal proof of the functional activity of reconstituted channel proteins in lipid bilayers is to show modulation of channel activity by changing external parameters like selective binding of active molecules in the case of ligand-gated ion channels, changing the lateral membrane pressure in the case of mechano-sensitive channels or inducing a proper transmembrane potential in the case of voltage-gated ion channels. What is a stringent requirement in the field of BLM and patch-clamp experiments, is unfortunately only rarely acquired in the case of channels in supported or tethered lipid membranes. Very often a comparison of the electrical resistance of two entirely different samples, one composed of pure tethered lipid membranes and the other separately prepared sample of a tethered membrane comprising the channel protein is taken to proof channel activity if the second sample shows a decreased membrane resistance. It is rather difficult to exclude in this way simple bilayer defects introduced by protein insertion from true ion channel activities. We have found only a few cases where ligand gating has been demonstrated in a clear and specific dose–response manner. The first report concerns the gating of Gramicidin channels in tethered membranes by antibody binding to a chemically modified Gramicidin carrying an antigen for the mentioned antibody [44]. Besides this elegant concept of immunosensing with small ionophores, we have found only two more cases where the resistance of tethered lipid membranes was modulated in a dose response manner, one for OmpF [45] and another one for SLIC [32,46]. The electrical resistance of SLIC-containing lipid bilayers was shown to increase in the presence of nanomolar concentrations of the antibody Sp3E9 that has been designed to recognize the NANP sequence. Unspecific adsorption of IgG to these layers was found to be small and could be subtracted quantitatively [32].

The incorporation of SLIC in a preformed tethered lipid layer was reflected in a drop in membrane resistance measured on the real part of the impedance at 0.01 Hz (Fig. 4A). Upon addition of SLIC in the aqueous phase the layer resistance decreases immediately and saturates in about 30 min. The slow kinetics allows interruption of the insertion process of the protein into the lipid bilayer by washing with buffer and thus keeping the number of SLIC molecules in the membrane as low as possible in a controlled way. Selective antibody binding to SLIC in the lipid bilayer increases the membrane resistance as a function of the concentration of the antibody Sp3E9 in the aqueous phase (Fig. 4B). Taken into account a conductance of 90 pS measured in freestanding black lipid membranes, the observed responses correspond to the incorporation of 200 open SLIC channels and the total closure of 95 channels in the tethered lipid bilayer [46]. With the presently achieved signal-to-noise ratio it will be possible to detect the closure of a few individual channels.

Ligand binding can also be measured in combination with other techniques. The interaction between the R-domain of colicin N with OmpF containing lipid bilayers has been measured by conductance measurements in black lipid membranes and by impedance spectroscopy and SPR in tethered lipid bilayers. A good agreement between the dose–response curves obtained with these techniques was obtained (Fig. 5).

2.3. Impedance spectroscopy

Electrical impedance spectroscopy can be performed in several ways [57]. The data presented here have been obtained by using a 2-phase-channel lock-in amplifier such as SR 850 from Stanford Research Systems. Sinusoidal voltages of 10 mV amplitude (root-mean-square) were applied to the electrochemical cell by

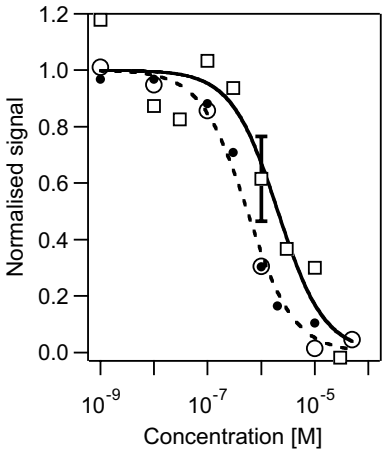

Fig. 5. Interaction between OmpF in lipid membranes and Colicin N added at different concentrations to the surrounding buffer solution: conductance of OmpF in BLMs (●); impedance of OmpF in tethered membranes (□); surface plasmon resonance signal due to binding of Colicin N to OmpF in tethered membranes (○) (reprinted with permission from reference [45]).

the internal function generator in a programmable automated frequency sweep. The currents in phase and 90° out of phase with the applied AC voltage are directly recorded on the two channels of the lock-in amplifier and a highly accurate phase-sensitive detection was performed digitally. Our set-up included a home-built current-to-voltage converter with a gain of 10^4 to 10^7 and the lock-in amplifier measured the input voltage. An additional external function generator or a DC offset can be used. The measurement of highly electrically insulating layers required the use of high and low amplification gains at low and high frequencies of the impedance spectrum, respectively.

An impedance spectrum will include contributions from the whole electrochemical cell, i.e. the electrodes, the interfaces and the electrolyte. It is good practice to minimize the effect of all elements except the working electrode. Therefore, a large (ca. 1 cm^2 effective area) and highly conductive counter electrode should be used. If the electrolyte contains chloride ions, an AgCl-coated Ag wire is recommended. High concentration of electrolyte (usually KCl $\geqslant$ 0.1 M) decreases the effect of the electrical resistance of the aqueous phase and of the interfacial capacitances. Under these conditions, the impedance of a small working electrode coated with an electrically insulating lipid layer will dominate the spectrum. An electrochemical system with two electrodes is sufficient because only a negligible current will actually flow through the Ag/AgCl electrode.

2.4. Inside-out cell membrane sheets supported on planar supports

Various procedures have been developed to immobilize inside-out membrane sheets (the inner leaflet of the cell membrane is exposed to the solution) on planar surfaces. These include the rupture of adherent cells by sonication [58] and lysis [59], or the spontaneous fusion in the case of erythrocytes [60]. Recently, we showed that large membrane sheets (>100 μm^2) can be detached from the plasma membrane of adherent living cells and transferred onto planar glass surfaces [61,62]. These supported native cell membranes offer interesting novel possibilities for investigating the lateral distribution of membrane proteins and lipids, and their mutual interactions during biochemical membrane processes by ensemble and single molecule fluorescence techniques; in the case of activation of channel proteins, the planar membranes are ideally suited to combine fluorescence with planar patch clamp experiments [61–64].

2.4.1. Preparation of membrane sheets

Human embryonic kidney (HEK-293) cells were grown in DMEM-F12 medium in six-well plates pre-incubated with 0.1 mg/mL solution of poly-L-lysine (PLL) in PBS for 1 h. Highest yield of large membrane sheets was obtained using cells at 30–40% confluence. Cleaned and dried 0.17 mm glass coverslips were treated by oxygen plasma (Harrick, plasma cleaner) for 15 min, incubated with 0.1 mg/mL PLL in PBS for 20 min and washed with PBS. HEK cells were rinsed with PBS and pressed with a PLL-coated coverslip for 3–4 min to create good contact between the upper membrane of the cells and the glass surface. Care was taken to avoid lateral movement of the coverslip during application and removal in order to prevent damage or detachment of membrane sheets. In some experiments, the cells were covered with deionized water prior of being sandwiched between the glass plates. The glass coverslip was then removed ripping off the upper cell membranes, washed with PBS and mounted on a measurement chamber filled with PBS.

2.4.2. Protein labeling

Cell membrane sheets were prepared from HEK cells expressing various representative membrane proteins involved in important signal transduction pathways: the α1b-adrenergic receptor (α1b-AR) [61] and the neurokinin-1 receptor (NK1R) [64] as prototypical G protein-coupled receptors (GPCRs), G proteins as membrane-anchored proteins [62], and the serotonin type 3 receptor (5HT3R) as a representative of ligand-gated ion channels (LGICs) [61,64]. Different labeling strategies have been used in order to characterize the proteins with fluorescent techniques: (i) the fusion to autofluorescent proteins, (ii) fluorescent analogues of ligands, (iii) fluorescent antibodies binding to selective epitopes on the target protein. The NK1R was genetically fused at its intracellular C-terminus with the green fluorescent protein, yielding the fusion receptor NK1R-GFP [65]. Each of the five subunits of the homopentameric 5HT3R was labeled with a cyan fluorescent protein (CFP) inserted into the cytoplasmic loop, yielding the 5HT3R-CFP, as described elsewhere [66]. The synthesis of the fluorescent analogue of the 5HT3R-specific ligand GR-Cy3 was previously described [67].

2.4.3. Confocal imaging

The measurement chamber was placed on the stage of an inverted scanning confocal microscope (LSM510, Zeiss) equipped with a 63 × water immersion objective of 1.2 NA and 240 μm working distance (Zeiss). Measurements were done at room temperature using the pinhole at 2 Airy units. Fluorescence signal intensities were evaluated using Zeiss LSM software.

2.4.4. Accessibility and functionality of integral membrane proteins

Fig. 6A and B shows typical inside-out membrane patches of HEK cells expressing the 5HT3R-CFP. The composition of the original cell membrane is preserved as well as the fluidity of both membrane leaflets [61]. As illustrated in Fig. 1B, the orientation of membrane proteins relative to the surface is controlled by our procedure of transferring membrane sheets: the extracellular membrane leaflet is facing the support, while the cytoplasmic leaflet is exposed to the bulk aqueous phase. The accessibility of the cytosolic side of the receptors was demonstrated by labeling an intracellular recognition element (an autofluorescent protein or a FLAG-tag) with specific antibodies conjugated to a fluorescent dye [61,63]. Moreover, the lateral diffusion of cytosolic membrane-anchored G proteins could be monitored at the single molecule level [62]. These results show that supported membrane sheets are suited to investigate internal membrane processes with advanced biophysical techniques.

Investigating signal transduction mediated by membrane receptors such as GPCRs or LGICs in the supported cell membrane sheets requires also an unrestricted access to the extracellular binding site for ligand molecules. With the α1b-AR, the related antagonist prazosin (and its fluorescent derivative prazosin-Bodipy FL) and agonist epinephrine are membrane permeable, which allowed the conduction of ligand binding experiments and revealed the functionality of immobilized GPCRs [61]. However, the ability of a compound to cross the cell membrane depends on its physicochemical properties and in most cases the permeability is limited. As shown in Fig. 6B with cell membrane sheets containing the 5HT3R-CFP, addition of the fluorescent derivative of the antagonist GR-Cy3 leads to a crown-like labeling of the patches. This result indicates that only the binding sites of the peripherical receptors are accessible and that the fluorescent ligand cannot diffuse across the cell membrane in the time range of the experiments (∼1 h). In the presence of excess agonist quipazine the fluorescence signal disappears demonstrating the binding specificity. Similar labeling properties were observed with immobilized NK1R [63].

2.5. Inside-out cell membrane sheets supported on micrometer-sized beads

Micrometer-sized beads (polystyrene, latex, glass, silica, magnetic) are versatile templates for immobilizing biological objects, since they can easily be modified to carry different chemistries on

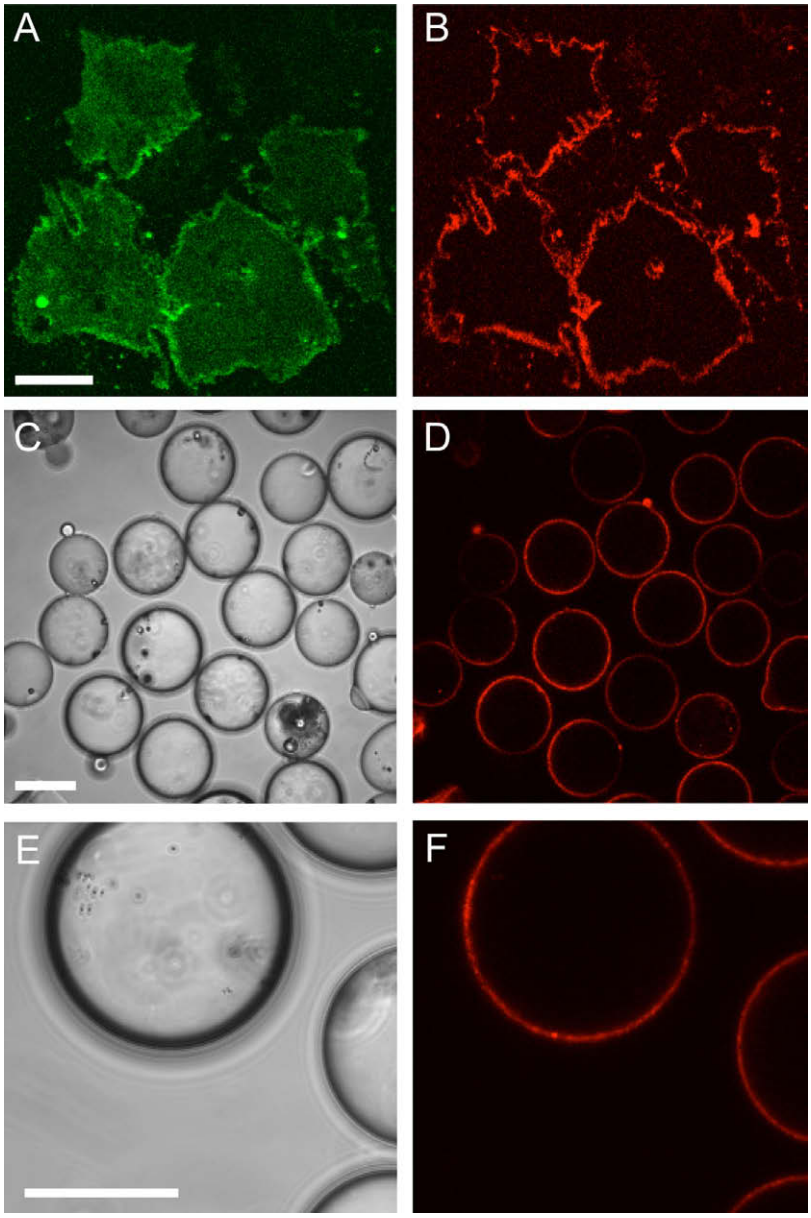

Fig. 6. (A,B) Confocal fluorescence microscope images of cell membrane sheets immobilized on a glass slide. (A) The membrane patches show fluorescence of the fusion protein 5HT3R-CFP expressed at the plasma membrane (excitation 458 nm/emission >475 nm). Scale bar: 10 μm. (B) After incubation with the 5HT3R-specific ligand GR-Cy3, only the receptors located at the periphery of the membrane sheets were labeled (excitation 543 nm/emission >560 nm). (C–F) Confocal fluorescence microscopy of plasma membrane-coated beads settled on a glass slide. The hydrophobic dye C_{18}-Cy5 was used for visualizing the cellular plasma membrane coating the beads (excitation 633 nm/emission >650 nm). Scale bars: 50 μm.

their surface. A wide variety of applications including immunoassays, affinity assays, DNA hybridization assays and protein–protein interactions at suspended or surface-immobilized beads have been developed since many years. Bead isolation techniques have been employed for plasma membrane purification providing a rapid tool for protein and phospholipid composition analysis [68–71]. For these applications, cultured cells were tightly attached to positively charged beads and disrupted to produce patches of plasma membranes whose cytoplasmic surface was exposed and accessible to the solution. Aiming at downscaling GPCR activation and downstream signaling analyses on beads, we improved existing procedures for preparing plasma membrane-coated glass beads.

2.5.1. Coating glass beads with cellular plasma membranes

A number of protocols have been proposed to isolate cell plasma membranes on glass [68], polyacrylamide [69], or DEAE-sephadex [70] beads. We prepared glass beads coated with inside-out plasma membranes from HEK cells by using a previously described procedure for cell attachment and removal [71] including some modifications. The time-consuming and costly procedure to create positive surface charges on the glass beads [68] was replaced by a rapid treatment reducing the whole procedure to 1 h. Acid-washed glass beads ($\leqslant$106 μm, Sigma) were treated by oxygen plasma for 1 min to activate the surface and incubated in 0.1 mg/mL solution of polylysine for 10 min under gentle shaking. Polylysine-coated beads were washed three times in low-ionic strength and isotonic buffer (attachment buffer: 140 mM sorbitol, 20 mM sodium acetate, pH 5). Live HEK cells were gently pelleted and resuspended in attachment buffer. A 50% (v/v) suspension of positively charged beads were added dropwise to the cells and incubated for 10 min under gentle agitation. The cell-attached beads were then washed three times in attachment buffer to remove unbound cells, followed by three-time washing in PBS pH

7.4. Disruption of cells and isolation of plasma membranes on beads were performed by vigorously vortexing the tube for 10 s to disperse the beads, followed by 20 s bath-sonication. Cytoplasmic organelles and debris were removed by washing three times the beads with PBS. Finally, the beads coated with patches of plasma membranes were stored at −20 °C. Attachment of cells and isolation of membranes were carried out on ice.

2.5.2. Imaging cell membrane sheets on beads by fluorescence microscopy

Plasma membrane-coated beads were settled on a 0.17-mm glass coverslip and analyzed by confocal microscopy in PBS at room temperature. Addition of the membrane dye C_{18}-Rho revealed the presence of cell membranes on the bead surface (Fig. 6C–F). No labeling was observed on the polylysine-coated beads harvested prior addition of cells (data not shown). The efficiency of cell adhesion and rupture is revealed by the high yield of labeled beads, the nearly completely covered surface per bead and the absence of cells remaining attached to the beads. Plasma membrane-coated beads could be stored at −20 °C or kept at 4 °C in PBS for days without loss of surface coverage, demonstrating that membranes are firmly attached to the beads. Because microcarrier beads can easily be transported and manipulated, our technique provides an ideal tool for miniaturization of functional assays down to the single bead level for probing interactions between membrane receptors like GPCRs and cytoplasmic effector proteins such as G proteins, β-arrestins and kinases. Moreover, functionalized microbeads can be trapped optically in a micro-array format for parallel bioanalysis of ligand binding or membrane receptor activation.

2.6. Hybrid supported/suspended cell membrane sheets across nanoapertures

In order to extend pharmacological studies of cell surface receptors on supported membranes, new technologies are required to overpass the limitation of membrane permeability for extracellular compounds. Our strategy of immobilizing cell membrane sheets on planar supports structured with arrays of submicrometer sized apertures (Fig. 1D) provides full accessibility to the intra- and extracellular sides of the membranes suspended across the holes [64].

2.6.1. Fabrication of the nanopore chips

Free-standing ($100 \times 100\,\mu m^2$) 100 nm, 200 nm and 500 nm thick low stress Si_xN_y supports were fabricated using standard procedures such as low pressure chemical vapor deposition, photolithography, and anisotropic KOH etching. The Si_xN_y film was then covered by photoresist and the nanopores were subsequently opened by electron-beam lithography and reactive ion etching. Finally the photoresist was removed by oxygen plasma. Focused-ion-beam (dual beam Nova 600 NanoLab, FEI Company) was also used for producing multi-aperture devices [72]. Patterns of 10×10 and 20×20 apertures with diameters of 100 to 600 nm and arrayed in 2 μm or 5 μm lattices have been fabricated with the above-mentioned techniques (Fig. 7).

2.6.2. Treatment of the silicon chips

After 1 h immersion of the chips in isopropanol, the organic solvent was replaced by deionized water. Water was then degassed by purging with argon for 30 min to remove air bubbles that might be entrapped in the nanopores. The chips stayed immersed in water overnight. Prior to the experiment, the chips were incubated for 20 min in a degassed aqueous solution of 0.1 mg/mL PLL and then washed with PBS. After each experiment, the chips containing cellular membranes were first washed with deionized water and isopropanol, and remaining organic contaminations were removed by oxygen plasma treatment for 15 min.

2.6.3. Preparing the hybrid supported/suspended plasma membranes

The general procedure for preparing hybrid supported/suspended cell membranes is the same as that described before for producing purely supported plasma membrane sheets on planar glass plates. After transferring the cell membrane sheets across the aperture arrays, the silicon chip was mounted into a polydimethylsiloxane chamber comprising a microchannel for exchanging fluidics. The horizontal configuration of the device and the narrow bottom channel were designed for enabling fluorescence microscopy with short working distance objectives.

2.6.4. Characterization of cell membrane sheets on nanoapertures

Cell membrane sheets with areas larger than $100\,\mu m^2$ can regularly be deposited onto the aperture arrays. Yields of transfer were higher for apertures with diameters <500 nm and separated by 5 μm. A typical example of an immobilized cell membrane sheet containing the NK1R-GFP is shown in Fig. 8. The periodic arrangement facilitates the localization of the nanopores covered by the membrane sheets. No alteration of the membrane fluorescence due to the presence of the apertures was detected within the spatial resolution of the confocal microscope (Fig. 8D). Intact hybrid supported/suspended planar cell membranes could be observed over days after transfer showing the long-term stability of the system. In addition, we demonstrated the accessibility to both

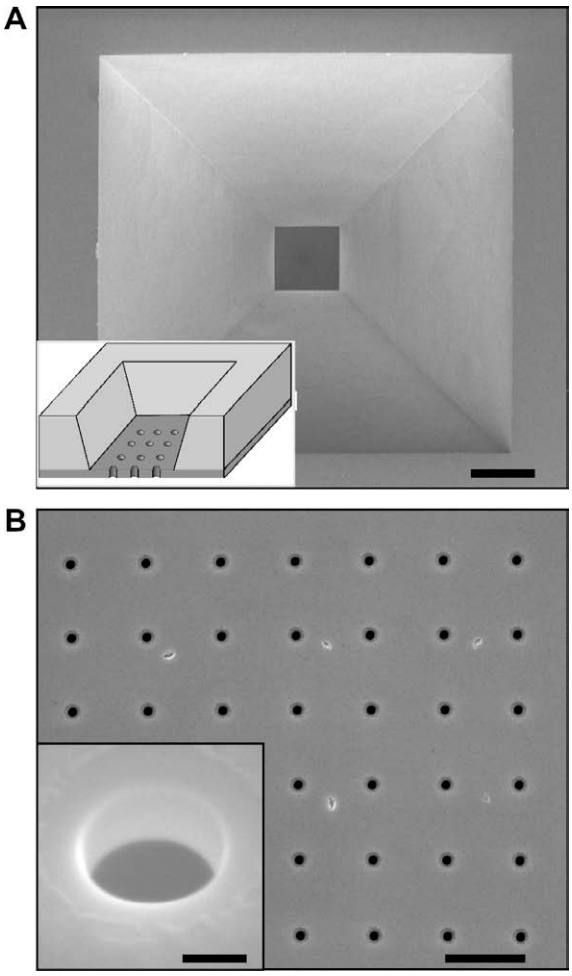

Fig. 7. (A) Scanning electron micrograph of the chip cavity and the free-standing silicon nitride film at the bottom. Scale bar: 100 μm. Inset: Schematic view of a silicon chip. (B) Scanning electron micrograph of a 5-μm lattice array of 500-nm-sized holes fabricated in a 500-nm thick silicon nitride film. Scale bar: 5 μm. Inset: Scanning electron micrograph of a single hole after tilting the sample to allow an obstructed view of the walls. Scale bar: 200 nm.

extracellular and intracellular surfaces of suspended membranes at the bottom of the nanopores by targeting membrane constituents side-specifically with fluorescent markers [64].

3. Conclusion and outlook

We reported here on recent electrical and optical techniques for investigating cellular signaling reactions in artificial and native membranes immobilized on solid (perforated) supports. Special emphasis was given to ionotropic and G protein-coupled receptors. Highly insulating tethered lipid bilayers on gold electrodes enable to electrically address the dose dependent activation of ligand-gated ion channels with well-defined membrane composition. Complementarily, native membranes isolated from living cells can be immobilized in a well-controlled orientation on microbeads and porous supports for exploring the reactivity of membranous components in their supramolecular environment. We believe that these technologies open new directions for investigating biological membranes, screening compounds for their capabilities to influence cellular membrane processes and in turn using membranes or membrane proteins as biosensors for detecting analytes. A few tempting possibilities are outlined in the following.

3.1. Tethered membranes with giga-ohm seals on gold electrodes

(1) SPR has been already used in combination with impedance measurements to probe the binding of choleratoxin to its ganglioside membrane receptors and its subsequent membrane insertion [46], and in the case of OmpF to monitor ligand binding and channel activity [45]. It would be interesting to combine electrical impedance measurements with other optical techniques such as Fourier transform infrared (FTIR) spectroscopy using gold-coated attenuated total reflection elements [73]; FTIR protein spectra would deliver information on conformational changes of channel proteins during activation [74].

(2) Another challenging approach would be to measure on tethered planar membranes simultaneously structural changes of and ion current flow across individual channel proteins by scanning probe techniques using for example electrically conducting cantilevers [9]. Scanning probe techniques such as atomic force microscopy offer atomic resolution of conformational changes during channel activation.

(3) Impedance spectroscopy would be also suited to detect activation of GPCRs. The activation of a GPCR by an external signal is very often followed by the activation of a ligand-gated ion channel in the downstream signaling cascade, which could be sensed by impedance spectroscopy. The prerequisites to realize a functional bioassay based on impedance spectroscopy are (i) to coexpress the corresponding GPCR with its downstream activatable ion channel, (ii) to transfer and tether the native cellular plasma membrane to the working gold electrode, and (iii) to use membrane permeable (hydrophobic) GPCR-activating ligands. Especially the last requirement is fulfilled in the case of odorant receptors: most of the active odorants are hydrophobic molecules. We therefore are confident that this biosensor concept will be ideally suited for the construction of an artificial nose.

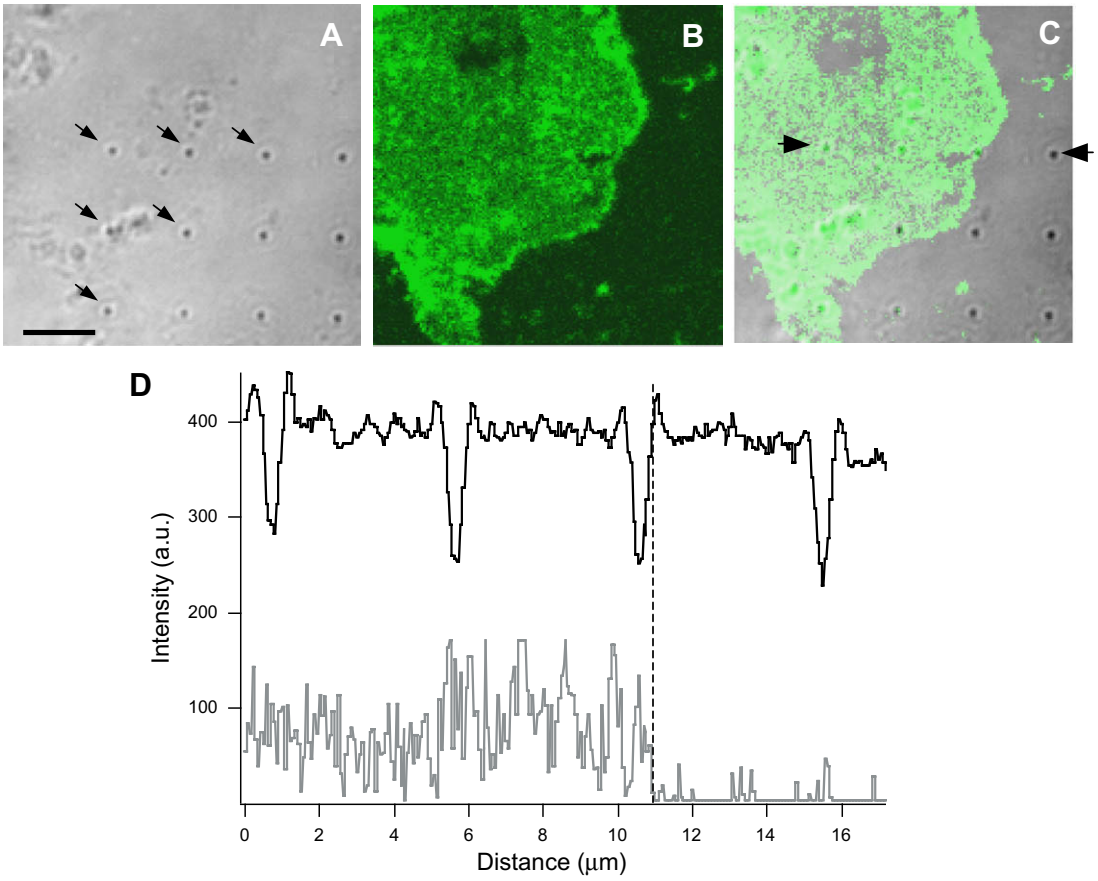

Fig. 8. (A–C) Confocal fluorescence images of native membrane patches derived from HEK cells expressing the fusion protein NK1R-GFP. Membrane sheets were transferred to a silicon microchip structured with 200 nm apertures arrayed on a 5-μm quadratic lattice (arrows in A). Nano-apertures are distinctly visualized on the transmission channel, while native membrane sheets are characterized on the fluorescence channel (excitation 488 nm/emission 505–530 nm). Scale bar: 5 μm. (D) Line intensity profile on the fluorescence channel (gray) and the transmission channel (black) between the two arrows depicted in (C). The dashed line indicates the edge of the membrane patch.

3.2. Future directions for cell membrane sheets on solid supports

(1) Optical (fluorescence) microscopy/spectroscopy offers possibilities to detect molecular reactions with single molecule resolution at, in and across cell membranes. For this approach we will use in the future a zero-mode waveguide configuration comprising apertures of subwavelength dimensions in a metal film [75]. Such a device is also suited for planar patch-clamp measurements to detect electrically single ion channel activities and monitor simultaneously conformational changes of the protein channel by fluorescence techniques [47,76–78]. Because the native membrane sheets across apertures can be accessed both from the exo- and from the cytoplasmic site it is possible to label different membrane components with distinguishable probes using novel orthogonal labeling techniques [79–82] and thus follow complex biochemical networks (extracellular part might be labeled in the living cells, intracellular regions after detaching membranes across the aperture). Of interest might be also the possibility to reconstitute signaling pathways by inserting lipid-anchored signaling proteins, such as G proteins [83] to the cytoplasmic side of the planar membrane sheet.

(2) Scanning probe techniques such as atomic force microscopy offer possibilities to monitor in situ the transduction of external signals across the cell membrane in terms of protein structural changes and lateral organization [84].

(3) Attaching living cells across nanopore arrays in solid supports offers the possibility to dispense locally activating compounds with (sub)micrometer sized lateral distribution to probe signaling reactions at different regions of a live cell.

(4) Our approach offers also possibilities for novel biosensing concepts using multiarrays of a large variety of cells and cellular organelles due to the long-term stability of planar native membranes. Many different cell sorts and/or receptor proteins might be probed simultaneously thereby either on supports or free-floating using multiple laser tweezers [85].

Acknowledgments

This work was supported by the European Commission via contract LSHG-CT-2004-504601 (E-MeP), the KTI-CTI and the Competence Centre for Materials Science and Technology (CCMX programme). We thank Luca Berdondini for assistance with microelectrode fabrication.

References

[1] R.G.W. Anderson, K. Jacobson, Science 296 (2002) 1821–1825.
[2] E. Meylan, J. Tschopp, M. Karin, Nature 442 (2006) 39–44.
[3] P.G. Strange, Curr. Opin. Drug Discov. Devel. 11 (2008) 196–202.
[4] D.J. Muller, N. Wu, K. Palczewski, Pharmacol. Rev. 60 (2008) 43–78.
[5] B. Kobilka, G.F.X. Schertler, Trends Pharmacol. Sci. 29 (2008) 79–83.
[6] F.M. Ashcroft, Nature 440 (2006) 440–447.
[7] Y.H.M. Chan, S.G. Boxer, Curr. Opin. Chem. Biol. 11 (2007) 581–587.
[8] R. Rigler, H. Vogel (Eds.), Single Molecules and Nanotechnology, vol. 12, Springer Series in Biophysics, 2008.
[9] D.J. Müller, K.T. Sapra, S. Scheuring, A. Kedrov, P.L. Frederix, D. Fotiadis, A. Engel, Curr. Opin. Struct. Biol. 16 (2006) 489–495.
[10] D.S. Majumdar, I. Smirnova, V. Kasho, E. Nir, X. Kong, S. Weiss, H.R. Kaback, Proc. Natl. Acad. Sci. USA 104 (2007) 12640–12645.
[11] E. Rhoades, E. Gussakovsky, G. Haran, Proc. Natl. Acad. Sci. USA 100 (2003) 3197–3202.
[12] M. Kessler, K.E. Gottschalk, H. Janovjak, D.J. Muller, H.E. Gaub, J. Mol. Biol. 357 (2006) 644–654.
[13] K.G. Suzuki, T.K. Fujiwara, F. Sanematsu, R. Iino, M. Edidin, A. Kusumi, J. Cell Biol. 177 (2007) 717–730.
[14] H.M. McConnell, T.H. Watts, R.M. Weis, A.A. Brian, Biochim. Biophys. Acta 864 (1986) 95–106.
[15] V. Vontscharner, H.M. McConnell, Biophys. J. 36 (1981) 421–427.
[16] L.K. Tamm, H.M. McConnell, Biophys. J. 47 (1985) 105–113.
[17] A.A. Brian, H.M. McConnell, Proc. Natl. Acad. Sci. USA 81 (1984) 6159–6163.
[18] E. Sackmann, Science 271 (1996) 43–48.
[19] J. Salafsky, J.T. Groves, S.G. Boxer, Biochemistry 35 (1996) 14773–14781.
[20] C. Dietrich, L.A. Bagatolli, Z.N. Volovyk, N.L. Thompson, M. Levi, K. Jacobson, E. Gratton, Biophys. J. 80 (2001) 1417–1428.
[21] L.K. Tamm, Curr. Top. Membr. 52 (2002) 191.
[22] J.T. Groves, S.G. Boxer, Acc. Chem. Res. 35 (2002) 149–157.
[23] A.P.F. Turner I. Karube G.S. Wilson (Eds.), Biosensors: Fundamentals and Applications, Oxford Science Publications, 1987.
[24] F. Scheller, F. Schubert, D. Pfeiffer, R. Hintsche, I. Dransfeld, R. Renneberg, U. Wollenberger, K. Riedel, M. Pavlova, M. Kühn, et al., Analyst 114 (1989) 653–662.
[25] U. Jönsson, L. Fägerstam, B. Ivarsson, B. Johnsson, R. Karlsson, K. Lundh, S. Löfås, B. Persson, H. Roos, I. Rönnberg, et al., Biotechniques 11 (1991) 620–627.
[26] M.A. Cooper, Nat. Rev. Drug Discov. 1 (2002) 515–528.
[27] H. Lang, C. Duschl, M. Graetzel, H. Vogel, Thin Solid Films 210 (1992) 818–821.
[28] H. Lang, C. Duschl, H. Vogel, Langmuir 10 (1994) 197–210.
[29] R. Naumann, A. Jonczyk, R. Kopp, J. Vanesch, H. Ringsdorf, W. Knoll, P. Gräber, Angew. Chem. Int. Ed. 34 (1995) 2056–2058.
[30] J. Spinke, J. Yang, H. Wolf, M. Liley, H. Ringsdorf, W. Knoll, Biophys. J. 63 (1992) 1667–1671.
[31] C. Bieri, O.P. Ernst, S. Heyse, K.P. Hofmann, H. Vogel, Nat. Biotechnol. 17 (1999) 1105–1108.
[32] S. Terrettaz, W.-P. Ulrich, R. Guerrini, A. Verdini, H. Vogel, Angew. Chem. Int. Ed. Engl. 40 (2001) 1740–1743.
[33] S. Heyse, T. Stora, E. Schmid, J.H. Lakey, H. Vogel, Biochim. Biophys. Acta 1376 (1998) 319–338.
[34] M.L. Wagner, L.K. Tamm, Biophys. J. 79 (2000) 1400–1414.
[35] E.K. Sinner, W. Knoll, Curr. Opin. Chem. Biol. 5 (2001) 705–711.
[36] M. Tanaka, E. Sackmann, Nature 437 (2005) 656–663.
[37] A. Janshoff, C. Steinem, Anal. Bioanal. Chem. 385 (2006) 433–451.
[38] E.T. Castellana, P.S. Cremer, Surf. Sci. Reports 61 (2006) 429–444.
[39] R. Naumann, E.K. Schmidt, A. Jonczyk, K. Fendler, B. Kadenbach, T. Liebermann, A. Offenhausser, W. Knoll, Biosens. Bioelectron. 14 (1999) 651–662.
[40] R. Naumann, T. Baumgart, P. Graber, A. Jonczyk, A. Offenhausser, W. Knoll, Biosens. Bioelectron. 17 (2002) 25–34.
[41] K. Seifert, K. Fendler, E. Bamberg, Biophys. J. 64 (1993) 384–391.
[42] B. Kelety, K. Diekert, J. Tobien, N. Watzke, W. Dörner, P. Obrdlik, K. Fendler, Assay Drug Dev. Technol. 4 (2006) 575–582.
[43] S. Heyse, O.P. Ernst, Z. Dienes, K.P. Hofmann, H. Vogel, Biochemistry 37 (1998) 507–522.
[44] B.A. Cornell, V.L.B. Braach-Maksvytis, L.J. King, P.D.J. Osman, B. Raguse, L. Wieczorek, R.J. Pace, Nature 387 (1997) 580–583.
[45] T. Stora, J.H. Lakey, H. Vogel, Angew. Chem. Int. Ed. Engl. 38 (1999) 389–392.
[46] S. Terrettaz, M. Mayer, H. Vogel, Langmuir 19 (2003) 5567–5569.
[47] C. Schmidt, M. Mayer, H. Vogel, Angew. Chem. Int. Ed. Engl. 39 (2000) 3137–3140.
[48] A.T.A. Jenkins, N. Boden, R.J. Bushby, S.D. Evans, P.F. Knowles, R.E. Miles, S.D. Ogier, H. Schönherr, G.J. Vancso, J. Am. Chem. Soc. 121 (1999) 5274–5280.
[49] S. Terrettaz, T. Stora, C. Duschl, H. Vogel, Langmuir 9 (1993) 1361–1369.
[50] S.M. Schiller, R. Naumann, K. Lovejoy, H. Kunz, W. Knoll, Angew. Chem. Int. Ed. Engl. 42 (2003) 208–211.
[51] M. Mayer, S. Terrettaz, L. Giovangrandi, T. Stora, H. Vogel, in: J.M. Cooper, A.E.G. Cass, (Eds.), Biosensors, 2nd ed., A Practical Approach Series, vol. 268, Oxford University Press, Oxford, 2003, pp. 153–184.
[52] S. Terrettaz, W.-P. Ulrich, H. Vogel, Q. Hong, L.G. Dover, J.H. Lakey, Protein Sci. 11 (2002) 1917–1925.
[53] I.K. Vockenroth, D. Fine, A. Dodobalapur, A.T.A. Jenkins, I. Köper, Electrochem. Commun. 10 (2008) 323–328.
[54] M.L.W. Ludden, A. Mulder, K. Schulze, V. Subramaniam, R. Tampe, J. Huskens, Chem. Eur. J. 14 (2008) 2044–2051.
[55] E.L. Schmid, A.P. Tairi, R. Hovius, H. Vogel, Anal. Chem. 70 (1998) 1331–1338.
[56] I.K. Vockenroth, P.P. Atanasova, A.T.A. Jenkins, I. Köper, Langmuir 24 (2008) 496–502.
[57] J.R. Macdonald (Ed.), Impedance Spectroscopy, Wiley, New York, 1987.
[58] T. Lang, M. Margittai, H. Hölzler, R. Jahn, J. Cell Biol. 158 (2002) 751–760.
[59] N. Hirai, S. Sonobe, T. Hayashi, Proc. Natl. Acad. Sci. USA 95 (1998) 15102–15106.
[60] M. Tanaka, A.P. Wong, F. Rehfeldt, M. Tutus, S. Kaufmann, J. Am. Chem. Soc. 126 (2004) 3257–3260.
[61] J.-B. Perez, K.L. Martinez, J.-M. Segura, H. Vogel, Adv. Funct. Mater. 16 (2006) 306–312.
[62] J.-B. Perez, J.-M. Segura, D. Abankwa, J. Piguet, K.L. Martinez, H. Vogel, J. Mol. Biol. 363 (2006) 918–930.
[63] C. Danelon, M.J. Jenke, C. Schreiter, G.M. Kim, J.-B. Perez, C. Santschi, J. Brugger, H. Vogel, CHIMIA 60 (2006) A754–A760.
[64] C. Danelon, J.-B. Perez, C. Santschi, J. Brugger, H. Vogel, Langmuir 22 (2006) 22–25.
[65] B.H. Meyer, K.L. Martinez, J.-M. Segura, P. Pascoal, R. Hovius, N. George, K. Johnsson, H. Vogel, FEBS Lett. 580 (2006) 1654–1658.
[66] E. Ilegems, H. Pick, C. Deluz, S. Kellenberg, H. Vogel, J. Biol. Chem. 279 (2004) 53346–53352.
[67] T. Wohland, K. Friedrich, R. Hovius, H. Vogel, Biochemistry 38 (1999) 8671–8681.
[68] D.I. Kalish, C.M. Cohen, B.S. Jacobson, D. Branton, Biochim. Biophys. Acta 506 (1978) 97–110.
[69] B.S. Jacobson, D. Branton, Science 195 (1977) 302–304.
[70] L.J. Gotlib, D.B. Searls, Biochim. Biophys. Acta 602 (1980) 207–212.

[71] B.S. Jacobson, Biochim. Biophys. Acta 600 (1980) 769–780.
[72] C. Danelon, C. Santschi, J. Brugger, H. Vogel, Langmuir 22 (2006) 10711–10715.
[73] M. Liley, T.A. Keller, C. Duschl, H. Vogel, Langmuir 13 (1997) 4190–4192.
[74] P. Rigler, W.P. Ulrich, R. Hovius, E. Ilegems, H. Pick, H. Vogel, Biochemistry 42 (2003) 14017–14022.
[75] M.J. Levene, J. Korlach, S.W. Turner, M. Foquet, H.G. Craighead, W.W. Webb, Science 299 (2003) 682–686.
[76] T. Ide, Y. Takeuchi, T. Yanagida, Single Mol. 3 (2002) 33–42.
[77] V. Borisenko, T. Lougheed, J. Hesse, E. Fureder-Kitzmuller, N. Fertig, J.C. Behrends, G.A. Woolley, G.J. Schutz, Biophys. J. 84 (2003) 612–622.
[78] G.S. Harms, G. Orr, M. Montal, B.D. Thrall, S.D. Colson, H.P. Lu, Biophys. J. 85 (2003) 1826–1838.
[79] E. Guignet, R. Hovius, H. Vogel, Nat. Biotechnol. 22 (2004) 440–444.
[80] A. Keppler, H. Pick, C. Arrivoli, H. Vogel, K. Johnsson, Proc. Natl. Acad. Sci. USA 101 (2004) 9955–9959.
[81] B.H. Meyer, J.-M. Segura, K.L. Martinez, R. Hovius, N. George, K. Johnsson, H. Vogel, Proc. Natl. Acad. Sci. USA 103 (2006) 2138–2143.
[82] A. Watzke, M. Gutierrez-Rodriguez, M. Köhn, R. Wacker, H. Schroeder, R. Breinbauer, J. Kuhlmann, K. Alexandrov, C.M. Niemeyer, R.S. Goody, H. Waldmann, Bioorg. Med. Chem. 14 (2006) 6288–6306.
[83] L. Brunsveld, J. Kuhlmann, K. Alexandrov, A. Wittinghofer, R.S. Goody, H. Waldmann, Angew. Chem. Int. Ed. Engl. 45 (2006) 6622–6646.
[84] R.P. Gonçalves, G. Agnus, P. Sens, C. Houssin, B. Bartenlian, S. Scheuring, Nat. Methods 3 (2006) 1007–1012.
[85] F. Merenda, J. Rohner, P. Pascoal, J.M. Fournier, H. Vogel, R.P. Salathé, Proc. SPIE 6483 (2007) .